10-27-2020

An Integrated Model of Magnetic Hysteresis, the Magnetomechanical Effect, and the Barkhausen Effect

David C. Jiles
Iowa State University, dcjiles@iastate.edu

Winnie Kiarie
Iowa State University, wmkiarie@iastate.edu

An Integrated Model of Magnetic Hysteresis, the Magnetomechanical Effect, and the Barkhausen Effect

Abstract

This paper reviews the ferromagnetic hysteresis, magnetomechanical and Barkhausen properties of magnetic materials and presents an integrated model to describe these effects and the underlying mechanisms that cause these effects. Hysteretic properties of ferromagnets such as permeability, coercivity, remanence and hysteresis loss are known to be sensitive to external factors including applied stress, temperature and heat treatment, and internal factors like residual strain, microstructure, grain size, and anisotropy and the presence of precipitates of a second phase, such as iron carbide in steels. It thus becomes imperative to characterize the effect of these factors on the hysteresis parameters. Currently, several models such as Preisach, Stoner-Wohlfarth and Jiles-Atherton are used to describe the magnetic hysteresis of ferromagnetic materials. We review here the quasistatic Jiles-Atherton hysteresis model which describes hysteresis in terms of domain wall motion enabling a connection to be made to the physical response of the magnetic material. This model has been extended to include the magnetomechanical effect and the Barkhausen effect in ferromagnetic materials. Theoretical work presented here provides a conceptual framework linking together these magnetic property measurements with model parameters and to the structure of the material.

Keywords

Magnetic hysteresis, Magnetization, Mathematical model, Magnetic properties, Magnetic domains, Ferromagnetic materials, Magnetic domain walls

Comments

This is a manuscript of an article published as Jiles, D. C., and W. Kiarie. "An Integrated Model of Magnetic Hysteresis, the Magnetomechanical Effect, and the Barkhausen Effect." *IEEE Transactions on Magnetics* (2020). DOI: 10.1109/TMAG.2020.3034208. Posted with permission.

An Integrated Model of Magnetic Hysteresis, the Magnetomechanical Effect, and the Barkhausen Effect

D.C. Jiles[1,2] and W. Kiarie[2]
[1] Department of Electrical & Computer Engineering
[2] Department of Materials Science & Engineering
Iowa State University, Ames, Iowa 50011, USA

This paper reviews the ferromagnetic hysteresis, magnetomechanical and Barkhausen properties of magnetic materials and presents an integrated model to describe these effects and the underlying mechanisms that cause these effects. Hysteretic properties of ferromagnets such as permeability, coercivity, remanence and hysteresis loss are known to be sensitive to external factors including applied stress, temperature and heat treatment, and internal factors like residual strain, microstructure, grain size, and anisotropy and the presence of precipitates of a second phase, such as iron carbide in steels. It thus becomes imperative to characterize the effect of these factors on the hysteresis parameters. Currently, several models such as Preisach, Stoner-Wohlfarth and Jiles-Atherton are used to describe the magnetic hysteresis of ferromagnetic materials. We review here the quasistatic Jiles-Atherton hysteresis model which describes hysteresis in terms of domain wall motion enabling a connection to be made to the physical response of the magnetic material. This model has been extended to include the magnetomechanical effect and the Barkhausen effect in ferromagnetic materials. Theoretical work presented here provides a conceptual framework linking together these magnetic property measurements with model parameters and to the structure of the material.

1. FERROMAGNETIC HYSTERESIS

All ferromagnetic materials exhibit hysteresis in the variation of magnetic flux density B with magnetic field H as shown in Fig.1. The hysteresis properties such as permeability, coercivity, remanence and hysteresis loss of these materials are known to be sensitive to various factors such as stress, strain, grain size, heat treatment and the presence of precipitates of a second phase, such as iron carbide in steels. The measurement of hysteresis yields independent material properties, each of which changes to some degree with stress, strain, and microstructure. It is known that several independent parameters are needed in general to separate effects of the stress state from microstructure, hysteresis measurement would seem to be ideally suited for the determination of the properties of steels because several independent properties can be obtained from one measurement.

Despite this economy of means, there are certain difficulties that need to be overcome with the magnetic hysteresis method. First, the problem of demagnetizing effects due to finite geometries needs to be addressed, since results which may appear to be due to changes in sample properties can be caused by geometric effects. Second, it has proved difficult to adequately model hysteresis in ferromagnets and therefore it has been difficult to interpret changes in the macroscopic hysteretic properties in terms of fundamental changes in microscopic sample properties such as microstructure and residual strain. Nevertheless, both hysteresis [1] and the Barkhausen effect [2] are much better understood now and this has greatly assisted interpretation of nondestructive evaluation results obtained with these two methods.

In Memoriam

This paper is dedicated to the memory of Professor David L. Atherton scientist, engineer and educator.

This article has been accepted for publication in a future issue of this journal, but has not been fully edited. Content may change prior to final publication. Citation information: DOI 10.1109/TMAG.2020.3034208, IEEE Transactions on Magnetics

1.1 THEORY OF FERROMAGNETIC HYSTERESIS

To develop a model that describes the magnetic properties of ferromagnetic materials, we will consider how the ideas developed so far can be brought together to provide an integrated theoretical model of hysteresis in ferromagnets. A few models are in use at present; these include the Preisach model [3] which uses an array of switching hysterons, and the Stoner-Wohlfarth model [4] which uses anisotropic rotational hysteresis, which strictly only applies to single-domain particles, but has often been used for modeling properties of hard magnetic materials. We will use a more recent model of hysteresis [5] based originally on domain-wall motion which, as we have mentioned previously, is the principal cause of hysteresis in multi-domain specimens. This model, also considers the effects of domain rotation since the essence of the model is the establishment of a relationship between energy dissipation ("losses") and change in magnetization. Noteworthy, the model is for quasistatic situations, however it has also be extended to account for frequency dependent ferromagnetic hysteresis curves [6].

1.1.1 Energy loss through wall pinning

As described previously, [5] consider a 180° domain wall of area A between two domains aligned parallel and antiparallel to a magnetic field $\boldsymbol{H}$. If the wall moves through a distance dx under the action of a field H the change in energy in joules due to this domain movement is

$$dE = -2\mu_0 \boldsymbol{M_s}\cdot\boldsymbol{H} A\, dx \qquad (1)$$

Where μ_0 is the permeability of free space and $\boldsymbol{M_s}$ is saturation magnetization. Suppose the pinning energy of a given pinning site for a 180° domain wall is $\mu_0\varepsilon_\pi$ and that in general the pinning energy ε_{pin} is proportional to the change in energy per unit volume caused by moving the wall,

$$\varepsilon_{\text{pin}} = \frac{1}{2}\varepsilon_\pi(1 - cos\,\phi) \qquad (2)$$

Where ϕ is the angle between the moments in the neighboring domains. This means that for any pinning site the energy dissipation caused by unpinning is proportional to the change in magnetization $\Delta M = M_s\,(1 - \cos\phi)$. Equation (2) gives an expression for the pinning energy of a given site as a function of angle ϕ. When $\phi = 0$ the pinning energy must go to zero since the wall no longer exists in a physical sense. In the case of a 180° wall $\varepsilon_{\text{pin}} = \varepsilon_\pi$.

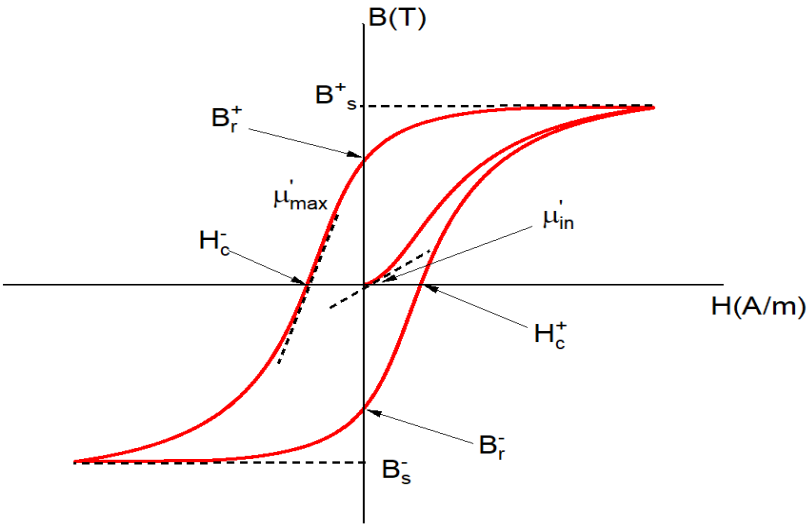

Fig.1. Typical hysteresis loop of a ferromagnetic material.

If there are *n* pinning sites per unit volume the energy dissipated by moving a 180°domain wall through a volume depends on the pinning energy ε_π, the number of pinning sites per unit volume n and the volume *Adx* swept out by the wall as it moves. In this case the energy dissipated in joules is

$$dE_{\text{loss}} = \mu_0 n \varepsilon_\pi A dx, \tag{3}$$

where *A* is the cross-sectional area of the wall. The change in magnetic moment will be

$$\mathrm{d}\boldsymbol{m} = 2\boldsymbol{M}_S A\, dx \tag{4}$$

where *Adx* represents the volume swept out by the movement of the domain wall. Therefore, the energy loss in joules per cubic meter will be

$$dE_{\text{loss}} = \frac{\mu_0 n \varepsilon_\pi \mathrm{d}\mathbf{m}}{2\boldsymbol{M}_S V} = \frac{\mu_0 n \varepsilon_\pi \mathrm{d}\boldsymbol{M}}{2\boldsymbol{M}_s} \tag{5}$$

where *V* is the volume, so that $d\boldsymbol{m}/V = d\boldsymbol{M}$. Replacing $(n\varepsilon_\pi/2\boldsymbol{M}_s)$ by the loss coefficient *k,* which represents the pinning, gives the energy loss per unit volume as

$$\mathrm{d}E_{\text{loss}} = \mu_0 k \mathrm{d}\boldsymbol{M} \tag{6}$$

which shows that the energy loss per unit volume is proportional to the change in magnetization.

1.1.2 Irreversible magnetization changes

Suppose the change in energy of a ferromagnet is manifested either as a change in magnetization or as hysteresis loss. Then we can write the energy equation as follows:

$$\begin{pmatrix}\text{Energy supplied to}\\ \text{material}\end{pmatrix} = \begin{pmatrix}\text{Change in}\\ \text{magnetostatic}\\ \text{energy}\end{pmatrix} + \begin{pmatrix}\text{Hysteresis}\\ \text{loss}\end{pmatrix} \tag{7}$$

In the case where there is no hysteresis loss, then the change in magnetostatic energy must equal the total energy supplied. When there is no hysteresis the magnetization follows the anhysteretic curve $\boldsymbol{M}_{\text{an}}(H)$

$$\mu_0 \int \boldsymbol{M}_{\text{an}}(\boldsymbol{H}) d\boldsymbol{H} = \mu_0 \int \boldsymbol{M}(\boldsymbol{H}) d\boldsymbol{H} + \mu_0 \int k \left(\frac{d\boldsymbol{M}}{d\boldsymbol{H}}\right) d\boldsymbol{H} \tag{8}$$

and differentiating with respect to H gives

$$\boldsymbol{M}_{\text{an}}(\boldsymbol{H}) = \boldsymbol{M}(\boldsymbol{H}) + k\left(\frac{d\boldsymbol{M}}{d\boldsymbol{H}}\right) \tag{9}$$

$$\frac{d\boldsymbol{M}}{d\boldsymbol{H}} = \frac{\boldsymbol{M}_{\text{an}}(\boldsymbol{H}) - \boldsymbol{M}(\boldsymbol{H})}{k} \tag{10}$$

This simple result states that the rate of change of magnetization $\boldsymbol{M}$ with field $\boldsymbol{H}$ is proportional to the displacement of the magnetization from the anhysteretic magnetization. That is the bulk magnetization $\boldsymbol{M}$ experiences a harmonic potential centered about $\boldsymbol{M}_{\text{an}}\,(\boldsymbol{H})$.

In fact, the situation is more complex than this in reality due to the internal coupling between the magnetic domains which is of the form envisaged by Weiss, so that the effective field becomes $\boldsymbol{H}_e = \boldsymbol{H} + \alpha\boldsymbol{M}$ resulting in the following equation, which we should note represents only the irreversible component of magnetization:

$$\frac{d\boldsymbol{M}_{\mathrm{irr}}}{d\boldsymbol{H}} = \frac{\boldsymbol{M}_{\mathrm{an}}(\boldsymbol{H}) - \boldsymbol{M}_{\mathrm{irr}}(\boldsymbol{H})}{k\delta - \alpha(\boldsymbol{M}_{\mathrm{an}}(\boldsymbol{H}) - \boldsymbol{M}_{\mathrm{irr}}(\boldsymbol{H}))} \tag{11}$$

Here δ is a directional term which has the value +1 for increasing magnetic field (d**H**/dt > 0), or -1 for decreasing magnetic field (d**H**/dt < 0), to ensure that the dissipation of energy due to hysteresis is always a loss, irrespective of the direction of change of field.

1.1.3 Reversible magnetization changes

In most cases both reversible and irreversible magnetization changes occur simultaneously. The reversible component of magnetization is due to reversible domain wall bowing, reversible translation and reversible rotation. In the model this has the form

$$\boldsymbol{M}_{\mathrm{rev}} = c(\boldsymbol{M}_{\mathrm{an}} - \boldsymbol{M}_{\mathrm{irr}}) \tag{12}$$

and since magnetization changes must be either reversible or irreversible, changes in the total magnetization $\mathbf{M}_{\mathrm{tot}}$ may be expected to be given by

$$\boldsymbol{M}_{\mathrm{tot}} = \boldsymbol{M}_{\mathrm{rev}} + \boldsymbol{M}_{\mathrm{irr}} \tag{13}$$

In fact, the form of the above equation is not very helpful since magnetization changes which begin as reversible can subsequently become "locked in" and end up as irreversible changes in $\boldsymbol{M}$. A much more useful expression is the differential equation that expresses the change in magnetization with field. In this case we can distinguish between a reversible contribution to the differential susceptibility and an irreversible contribution to the differential susceptibility, so that at any instant it is possible to say how much of the change in magnetization is being contributed by reversible or irreversible magnetization changes

$$\frac{d\boldsymbol{M}_{\mathrm{tot}}}{d\boldsymbol{H}} = \frac{d\boldsymbol{M}_{\mathrm{irr}}}{d\boldsymbol{H}} + \frac{d\boldsymbol{M}_{\mathrm{rev}}}{d\boldsymbol{H}} \tag{14}$$

Removing the subscript and assuming that whenever we talk about a change in magnetization without further qualification, we mean the total magnetization

$$\frac{d\boldsymbol{M}}{d\boldsymbol{H}} = \frac{(\boldsymbol{M}_{\mathrm{an}} - \boldsymbol{M}_{\mathrm{irr}})}{k\delta - \alpha(\boldsymbol{M}_{\mathrm{an}} - \boldsymbol{M}_{\mathrm{irr}})} + c\left(\frac{d\boldsymbol{M}_{\mathrm{an}}}{d\boldsymbol{H}} - \frac{d\boldsymbol{M}_{\mathrm{irr}}}{d\boldsymbol{H}}\right) \tag{15}$$

It is clear from this model that if $k \rightarrow 0$ then $\boldsymbol{M(H)} \rightarrow \boldsymbol{M}_{\mathrm{an}}\boldsymbol{(H)}$ which conforms with earlier comments that if there are no pinning sites the magnetization will follow the reversible anhysteretic magnetization curve. Solutions of this differential equation for various values of the model parameters are shown in Fig. 2.

This article has been accepted for publication in a future issue of this journal, but has not been fully edited. Content may change prior to final publication. Citation information: DOI 10.1109/TMAG.2020.3034208, IEEE Transactions on Magnetics

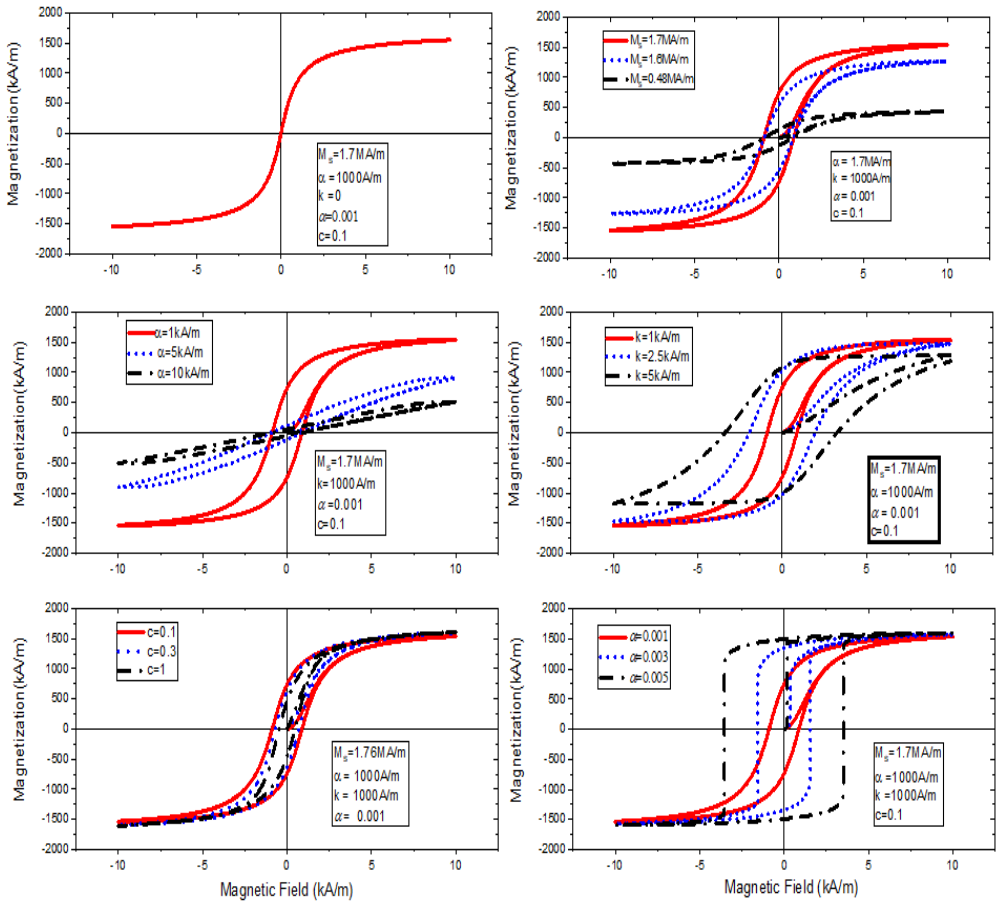

Fig. 2. Model hysteresis loops calculated using equation (15) derived in the JA model of hysteresis [5].

1.1.4 Relationship between hysteresis model coefficients and measurable magnetic properties

It is clearly important from the viewpoint of applications to be able to calculate the values of the various model parameters of hysteresis from the measured properties obtained from a magnetization curve. From equations (14) and (15) it can be shown that the initial differential susceptibility of the normal magnetization curve χ'_{in} is related to χ'_{the} differential susceptibility of the anhysteretic curve at the origin by the following equation [7]

$$\chi'_{\text{in}} = c\,\chi'_{\text{an}} \tag{16}$$

This agrees with Rayleigh's idea that χ'_{in} represents the reversible component of magnetization at the origin of the initial magnetization curve. In the case where k is constant and the reversible component c is negligible, that is $c \sim 0$, we have the following simple solution for k in terms of the coercivity $\boldsymbol{H}_c$ and the slope χ'_{Hc} of the hysteresis loop at H_c [8].

$$k = \boldsymbol{M}_{\text{an}}(\boldsymbol{H}_c)\left(\alpha + \frac{1}{\chi'_{\boldsymbol{H}_c}}\right) \tag{17}$$

when c $\neq$ 0 this equation becomes [8]

$$k = \boldsymbol{M}_{\text{an}}(\boldsymbol{H}_c)\left(\frac{\alpha}{(1-c)} + \left(\frac{1}{(1-c)\chi'_{\boldsymbol{H}_c} - c\frac{d\boldsymbol{M}_{\text{an}}(\boldsymbol{H}_c)}{d\boldsymbol{H}}}\right)\right) \tag{18}$$

This article has been accepted for publication in a future issue of this journal, but has not been fully edited. Content may change prior to final publication. Citation information: DOI 10.1109/TMAG.2020.3034208, IEEE Transactions on Magnetics

In the case of soft magnetic materials which have a low coercivity so that c is almost equal to 1 we can make some approximations which lead to a relation between k and H_c. For low coercivity materials the slope of the hysteresis loop at the coercive point χ'_{Hc} is approximately equal to the slope of the anhysteretic curve at the origin χ'_{an} and setting these quantities equal we have

$$\chi'_{an} = \chi'_{Hc} \tag{19}$$

$$\frac{\boldsymbol{M}_S}{3a-\alpha \boldsymbol{M}_S} = \frac{\boldsymbol{M}_{\mathrm{an}}(H_c)}{k-\alpha \boldsymbol{M}_{\mathrm{an}}(H_c)} \tag{20}$$

which leads to the following equation for k,

$$k = \frac{3a}{\boldsymbol{M}_s}(\boldsymbol{M}_{\mathrm{an}}(H_c) - \boldsymbol{M}_{\mathrm{irr}}(H_c)) \tag{21}$$

and $M_{irr} = 0$ at $H = H_c$

$$\boldsymbol{M}_{\mathbf{irr}}(\boldsymbol{H_c}) = 0 \tag{22}$$

So that

$$k = \frac{3a}{\boldsymbol{M}_s}(\boldsymbol{M}_{\mathrm{an}}(H_c) \tag{23}$$

Furthermore, the slope of the anhysteretic curve at the origin is quite linear and therefore, for small H_c we can write

$$\boldsymbol{M}_{\mathbf{an}}(\boldsymbol{H_c}) = \chi'_{an}\boldsymbol{H_c} = \left(\frac{\boldsymbol{M}_s}{3a-\alpha \boldsymbol{M}_s}\right)\boldsymbol{H_c} \tag{24}$$

and substituting this result into the expression for k gives

$$k = \frac{3a}{\boldsymbol{M}_s}\chi'_{an}\boldsymbol{H_c} = \frac{\boldsymbol{H_c}}{1-\left(\frac{\alpha \boldsymbol{M}_s}{3a}\right)} \tag{25}$$

This brings us to the important result that the coercivity H_c of a soft ferromagnetic material is determined principally by the pinning of domain-wall motion. In fact, $\boldsymbol{H_c} \simeq k$ for soft magnetic materials where $\alpha\mathbf{M_s} \ll \mathbf{3}a$.

1.1.5 Effects of microstructure and deformation on hysteresis

Changes in microstructure, in the form of additional magnetic inclusions such as second-phase particles with different magnetic properties from those of the matrix material, cause changes in the hysteresis properties by introducing more pinning sites that impede domain-wall motion and thereby leading to increased coercivity and hysteresis loss [9]. The same is also true of dislocations when their number density is increased by plastic deformation, either in tension or compression [10]. So, for example the addition of carbon into iron in the form of iron carbide particles increases coercivity and hysteresis loss. Cold-working of the material has a similar effect. The effect of these pinning sites is expressed via the coefficient k in the theory of ferromagnetic hysteresis. Clearly as their numbers increase k will increase proportionally and this results in an increase in the coercivity H_c as given in the equations above.

In the low-field limit the coercivity is $H_c \simeq k$ in units of A/m and consequently the coercivity is proportional to the product of the number density and average pinning energy per site.

This article has been accepted for publication in a future issue of this journal, but has not been fully edited. Content may change prior to final publication. Citation information: DOI 10.1109/TMAG.2020.3034208, IEEE Transactions on Magnetics

2. THE MAGNETOMECHANICAL EFFECT

The magnetomechanical effect is the name given to the phenomenon whereby application of stress causes a change in magnetization d**M**/dσ when there is no magnetic field present. This is the opposite to magnetostriction whereby the application of a magnetic field H causes strain in a material dλ/d**H** when there is no stress present. The magnetomechanical effect can be conveniently divided into two separate but related phenomena: the behavior of a material under constant stress and varying field (the 'isostress' case) and the behavior under constant field and varying stress (the 'isofield' case). In the isostress case, where a magnetic material is subjected to a uniaxial applied stress, the effect of the stress can be treated in some respect like an effective magnetic field which changes the anisotropy of the material.

2.1Effects of stress on bulk magnetization

Following classical thermodynamics of reversible systems, the Gibbs energy per unit volume is

$$G = U - TS + \frac{3}{2}\sigma\lambda, \tag{26}$$

in Joules per cubic meter, where λ is the bulk magnetostriction, σ is the stress, U is the internal energy per unit volume, T is the thermodynamic temperature and S is the entropy. The Helmholtz energy per unit volume is

$$A = G + \mu_0 \boldsymbol{HM}, \tag{27}$$

where H is the magnetic field and M is the magnetization. The internal energy U due to coupling of magnetic moments to the magnetization is

$$U = \frac{1}{2}\alpha\mu_0 \boldsymbol{M}^2 \tag{28}$$

The total effective field is given by

$$\boldsymbol{H}_{\text{eff}} = \left(\frac{1}{\mu_0}\right)\left(\frac{dA}{d\boldsymbol{M}}\right) \tag{29}$$

assuming the material is under a constant stress σ we can write the effective magnetic field H_σ due to the applied stress as

$$\boldsymbol{H}_{\text{eff}} = \boldsymbol{H} + \alpha\boldsymbol{M} + \boldsymbol{H}_{\boldsymbol{\sigma}} \tag{30}$$

$$\boldsymbol{H}_{\text{eff}} = \boldsymbol{H} + \alpha\boldsymbol{M} + \frac{3\sigma}{2\mu_0}\left(\frac{d\lambda}{d\boldsymbol{M}}\right) \tag{31}$$

where H is the magnetic field, αM is the mean-field coupling to the magnetization and H_σ is the equivalent magnetic field due to stress [11].

$$\boldsymbol{H}_{\sigma} = \frac{3\sigma}{2\mu_0}\left(\frac{d\lambda}{d\boldsymbol{M}}\right) \tag{32}$$

This can be used to determine the reversible magnetization under the action of an applied stress. For example, the anhysteretic magnetization curve, which is a reversible magnetization curve, can be determined by adding the stress equivalent field H_σ to the sum of the true field H and the internal coupling field αM due to interactions between the magnetic moments and the bulk magnetization.

This article has been accepted for publication in a future issue of this journal, but has not been fully edited. Content may change prior to final publication. Citation information: DOI 10.1109/TMAG.2020.3034208, IEEE Transactions on Magnetics

By way of example the Frohlich-Kennelly relation can be used with $\alpha M = 0$ (the Frohlich-Kennelly equation does not contain any explicit coupling of magnetic moments **m** to the magnetization **M**) to show the action of a stress σ the anhysteretic magnetization becomes

$$\boldsymbol{M}_{\mathrm{an}}(\boldsymbol{H}) = \frac{\beta\left(\boldsymbol{H}+\frac{3\sigma}{2\mu_0}\left(\frac{d\lambda}{d\boldsymbol{M}}\right)\right)}{1+\beta\left(\boldsymbol{H}+\frac{3\sigma}{2\mu_0}\left(\frac{d\lambda}{d\boldsymbol{M}}\right)\right)}\boldsymbol{M}_{\boldsymbol{S}} \tag{33}$$

This result shows how the anhysteretic magnetization is altered under the action of a constant applied stress σ for a material with positive magnetostriction derivative $d\lambda/\mathbf{dM}$. For large positive values of H, σ and $d\lambda/d\mathbf{M}$ the anhysteretic magnetization curve $\mathbf{M}_{an}(\mathbf{H})$ has an upper limiting value of $\mathbf{M}_{s}$. **.** Note that strictly speaking this analysis applies only to a reversible process.

In the case of both irreversible and reversible processes, the thermodynamic relationships become more complicated. However, the effect of constant applied stress on magnetic hysteresis loops can be calculated using a suitable magnetic model as shown in Fig. 3.

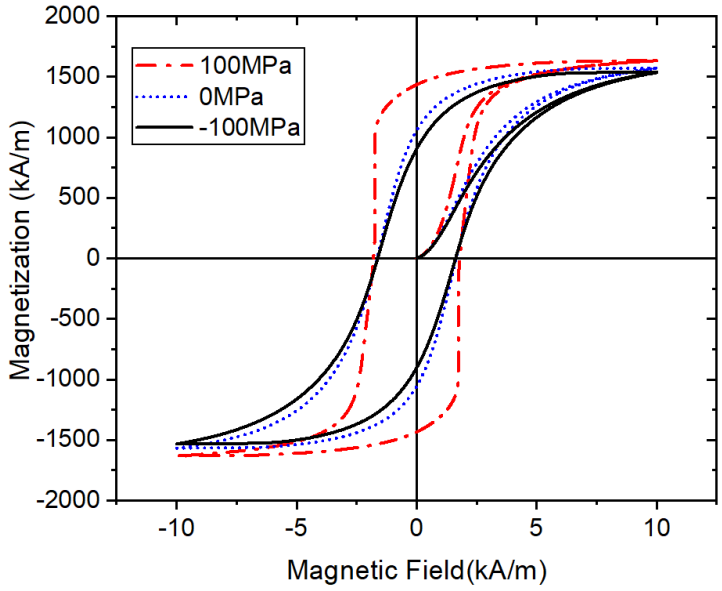

Fig. 3: Effect of constant stress on magnetic hysteresis loops based on the magnet -omechanical extension of the JA model.

2.2 Effect of Constant Stress on Maximum Differential Susceptibility

Based on the Jiles-Atherton mean field model for the anhysteretic magnetization Garikepati et al. [12] were able to combine that with the equation for the stress equivalent field H_σ equation (32) using the approximate relation $\lambda = bM^2$, so that

$$\boldsymbol{H}_{\sigma} = \frac{3b\sigma}{\mu_0}\boldsymbol{M} \tag{34}$$

which leads to an equation for the dependence of the reciprocal of the maximum differential susceptibility χ'_{max} on stress

$$\frac{1}{\left(\chi' max(0)\right)_{\boldsymbol{H}=0}} - \frac{1}{\left(\chi' max(\sigma)\right)_{\boldsymbol{H}=0}} = \frac{3b\sigma}{\mu_0} \tag{35}$$

This article has been accepted for publication in a future issue of this journal, but has not been fully edited. Content may change prior to final publication. Citation information: DOI 10.1109/TMAG.2020.3034208, IEEE Transactions on Magnetics

where b is a coefficient of proportionality linking magnetostriction λ to magnetization **M**, according to the approximate relation $\lambda = bM^2$. In many cases the maximum differential susceptibility χ'_{max} occurs at the coercive point H_c and note that $\chi'_{max} = \chi'_{Hc}$ .Equation (35) was verified experimentally, as shown in Figs. 4(a) and 4(b).

a) b)

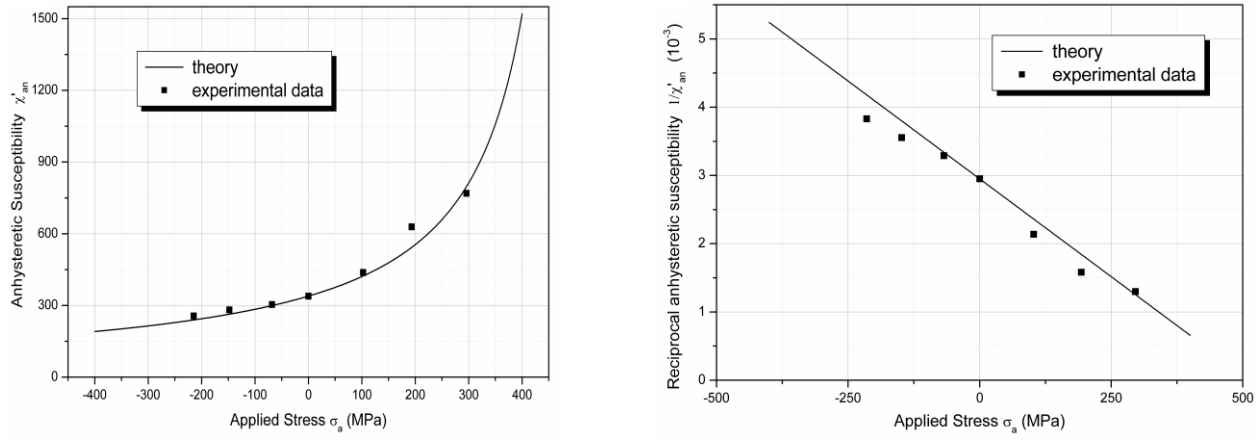

Fig. 4(a) Anhysteretic susceptibility at the origin as a function of stress, 4(b) Reciprocal anhysteretic susceptibility at the origin as a function of applied stress after Garikepati et al. [12].

2.3 Effect of Direction on the Stress Equivalent Field

Later the model equation (34) was extended to cover the case of a uniaxial stress at an arbitrary direction to the applied magnetic field by Kaminski, Jiles and Sablik [13] who developed an expression for the angular dependence of the effective field due to an applied uniaxial stress. This is shown in equation (36)

$$\boldsymbol{H}_\sigma(\theta) = \frac{3}{2}\frac{\sigma}{\mu_0}(cos^2\,\theta - \nu\, sin^2\,\theta)\left(\frac{\partial\lambda}{\partial \boldsymbol{M}}\right) \tag{36}$$

where σ is the stress, θ is the angle between the stress axis and the direction of $\boldsymbol{H_a}$, and ν is Poisson's ratio.

2.4 Effect of Variable Stress at Constant Field

In the isofield case the situation is more complicated, but Jiles [14] has shown that there are basic principles behind the change in magnetization with stress at constant field, $(\partial M/\partial\sigma)_H$, which can be used to derive the equation governing the mechanism. In this case the guiding principle is the law of approach of the magnetization toward the anhysteretic curve when the applied stress is changed. For the reversible component of magnetization the differential equation is

$$\frac{d\boldsymbol{M}_{\text{rev}}}{d\boldsymbol{W}} = c\left(\frac{d\boldsymbol{M}_{\text{an}}}{d\boldsymbol{W}} - \frac{d\boldsymbol{M}_{\text{irr}}}{d\boldsymbol{W}}\right) \tag{37}$$

where W is the elastic energy resulting from the applied stress σ, $W = \boldsymbol{\sigma}^2/2E$, that is the energy which causes the domain walls to break away from their pinning sites, and E is Young's modulus. For the irreversible component of magnetization

$$\frac{d\boldsymbol{M}_{\text{irr}}}{dW} = \frac{1}{\xi}(\boldsymbol{M}_{\text{an}} - \boldsymbol{M}_{\text{irr}}) \tag{38}$$

where now ξ is simply a decay coefficient, which relates the derivative of the irreversible magnetization with respect to elastic energy to the displacement of the irreversible magnetization from the anhysteretic. Here ξ has dimensions of energy per unit volume. When these two equations are combined, an expression for the derivative of the total magnetization with respect to elastic energy can be obtained:

$$\frac{d\boldsymbol{M}}{dW} = \frac{1}{\xi}(\boldsymbol{M}_{\text{an}} - \boldsymbol{M}) + c\frac{d\boldsymbol{M}_{\text{an}}}{dW}. \tag{39}$$

This last equation conveniently expresses the underlying law of the magnetomechanical effect in its simplest form the "law of approach to the anhysteretic". The equation can be used to calculate the rate of change of magnetization with stress under a variety of situations. It should be noted that $\boldsymbol{M}_{\text{an}}$ is itself stress dependent, and this stress dependence can be determined by incorporating the addition of an effective field term caused by stress $\boldsymbol{H}_{\sigma}$ into the equation for the anhysteretic. Therefore, when the magnetization approaches the anhysteretic under the action of an applied stress, it is approaching a moving target.

Changes in magnetic properties with stress cycling have been used to predict fatigue life of specimens by Shah and Bose [15]. It was found that the hardness of the specimens, which can be inferred from coercivity measurements, began to change long before any crack appeared.

3. THE BARKHAUSEN EFFECT

The Barkhausen effect is the phenomenon whereby discontinuous changes in the flux density ***B*** within a ferromagnet as the magnetic field ***H*** is changed continuously as shown in Fig. 5 This was first observed by Barkhausen [16] when a secondary or "pick up" coil was wound on a piece of iron and connected to an amplifier and loudspeaker. As the ***H*** field was increased smoothly a series of clicks were heard over the loudspeaker which were due to small voltage pulses induced in the secondary coil. These voltages were caused through the law of electromagnetic induction by small changes in flux density through the coil, arising from discontinuous changes in magnetization ***M*** and hence in the magnetic induction ***B.***

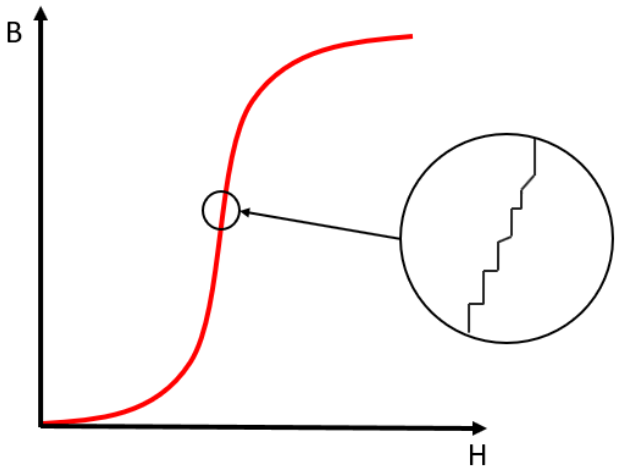

Fig. 5. Discontinuous changes in the magnetic flux density ***B*** as the magnetic field ***H*** is changed continuously

If the initial magnetization curve, which looks to be a smooth variation of B with H under normal circumstances, is greatly magnified, then the discontinuous changes in ***B*** which constitute the Barkhausen effect can be observed directly as in Fig.5. At first these discontinuities in induction were attributed to sudden discontinuous rotation of the direction of magnetization within a domain, a mechanism known as domain rotation, but it is now known that discontinuous domain boundary motion

This article has been accepted for publication in a future issue of this journal, but has not been fully edited. Content may change prior to final publication. Citation information: DOI 10.1109/TMAG.2020.3034208, IEEE Transactions on Magnetics

is the most significant factor contributing to Barkhausen emissions [18]. Nevertheless, both mechanisms do occur and contribute to the Barkhausen effect.

Fig. 6. shows a typical measured Barkhausen emission signal which is acquired as a voltage signal versus time. The maximum of the Barkhausen voltage occurs when the rate of change of B with time reaches a maximum. For a constant dH/dt this occurs at the coercivity H_c for most ferromagnets (see equation (40).

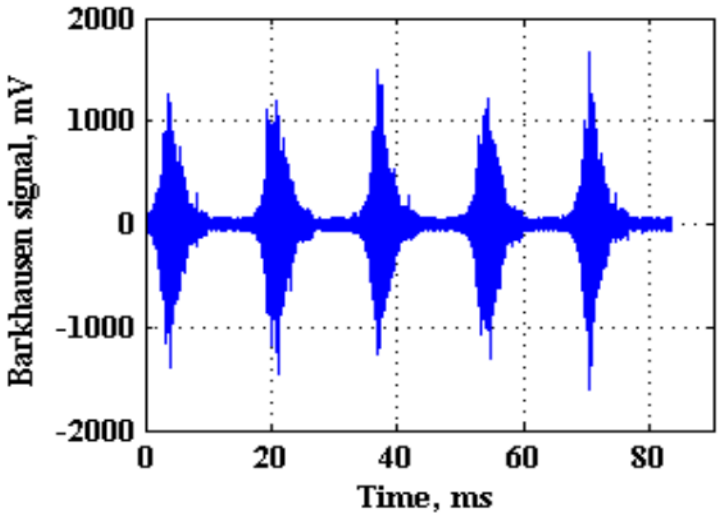

Fig. 6. Typical measured Barkhausen emissions shown as voltage against time [17].

For the calculated Barkhausen emissions $d\mathbf{M}_{JS}/dt$, according to the model, the voltage produced as shown in Fig. 7, is a result of various parameters including γ which represents the fraction of the irreversible magnetization change which occurs as Barkhausen events, the rate of change of the irreversible magnetization with magnetic field $d\mathbf{M}_{irr}/d\mathbf{H}$, the rate of change of magnetic field with time $\mathbf{dH}/dt$, the number of turns in the secondary or detection,coil, the cross sectional area of the coil and the rate of change of flux density with time $d\mathbf{B}/dt$ (see equation 40). The Barkhausen emissions are given here in arbitrary units.

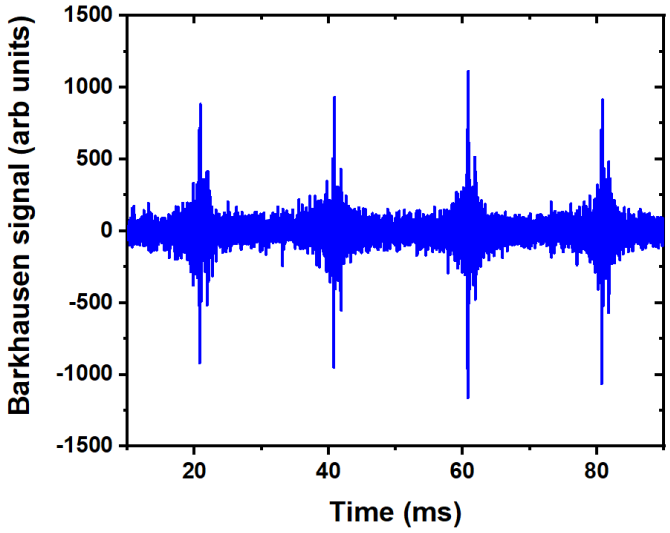

Fig. 7 Calculated Barkhausen emissions shown as voltage against time based on the extension of the JA model

3.1 THEORY OF THE BARKHAUSEN EFFECT

The quantitative description of the Barkhausen effect, at least in terms of defining equations, has proved to be difficult mainly because of its stochastic nature. Nevertheless, progress has been made, most notably by Bertotti et al. [19] who developed a comprehensive model of the effect based on stochastic processes. In this description the Barkhausen activity depends on the 'local potential' felt by the magnetic domain walls as they move through the material. This local potential Ep generates a localized magnetic field $H_p = dEp/dx$ which the domain walls need to overcome in order to move on. As shown in Fig. 8 the local potential has a random nature but provided the spatial extent is finite any stochastic function can be characterized by the combination of its average amplitude and its average wavelength. These fluctuations can be characterized on average, and these two parameters account for the number and intensity of Barkhausen emissions when subjected to a changing applied external field **H**.

Discontinuous changes in the flux density **B** occur as the wall jumps between the potential wells. For example in the one dimensional representation of the internal potential shown in Fig. 8, application of an increasing magnetic field causes the domain wall to rise reversibly up the side of the potential well until it reaches the maximum. The domain wall then jumps irreversibly to the next potential well by a Barkhausen jump as depicted by the arrows at the top of the potential well pinning sites. This process then continues with movements consisting of reversible wall motion of the domain walls within a potential well pinning site and irreversible domain wall motion as it jumps to the next potential well pinning site.

From the solution of the model equations, it is found that for a given rate of change of magnetization with time the Barkhausen activity in a given time interval is correlated with the activity in the previous time interval, but varies by an amount which is random in nature. Depending on the magnitude of this random component, the fluctuations in Barkhausen activity may be greater or less, with correspondingly less or more correlation with the activity in the previous time interval. The results of these model calculations agree well with experimental observations, which confirms the basic ideas behind the theory. An extension of the model by Jiles, Sipahi and Williams [20] has shown that the Barkhausen effect can be described in terms of two components: a deterministic component which is reproducible and depends on the differential susceptibility, and a stochastic component which is not reproducible.

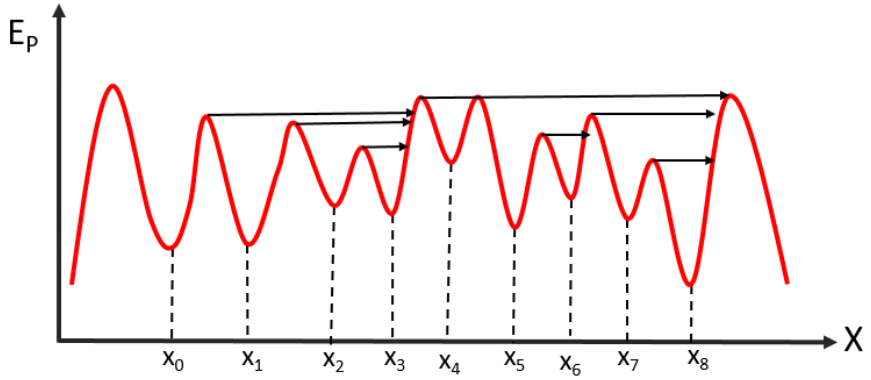

Fig.8. Random fluctuations in the local pinning field with position x_0 to xn as seen by a domain wall as it moves inside a magnetic material. Each minimum act as a pinning site, the pinning strength of which depends on the depth of the minimum. The domain walls jump irreversibly to the next potential well by a Barkhausen jump as depicted by the arrows.

The discontinuous changes in flux density, known as Barkhausen jumps, are caused mostly by sudden irreversible motion of magnetic domain walls when they break away from pinning sites as a result of

This article has been accepted for publication in a future issue of this journal, but has not been fully edited. Content may change prior to final publication. Citation information: DOI 10.1109/TMAG.2020.3034208, IEEE Transactions on Magnetics

changes in the applied magnetic field $\boldsymbol{H}$ [21]. The frequency range of Barkhausen emissions for NDE (nondestructive evaluation) purposes is usually 10-500 kHz, which means that detected emissions originate only from the surface layer of the test sample. The Barkhausen pulse height distribution, which is the number of events plotted against pulse height as shown in Fig.9, is dependent on the number density and nature of pinning sites within the material. These may be grain boundaries, dislocations, cavities, cracks or precipitates of a second phase material with different magnetic properties from the matrix material.

The connection between the Barkhausen effect and hysteresis was explored by Jiles, Sipahi, and Williams and subsequently by Jiles and Suominen [22]. In these studies, it was conjectured that the Barkhausen activity $d\mathbf{M}_{JS}/dt$ was proportional to the product of the differential susceptibility $d\mathbf{M}_{irr}/d\mathbf{H}$ and the rate of change of field $d\mathbf{H}/dt$. In addition, the Barkhausen effect signals are determined by other factors, since not all irreversible changes in magnetization are necessarily the result of Barkhausen events.

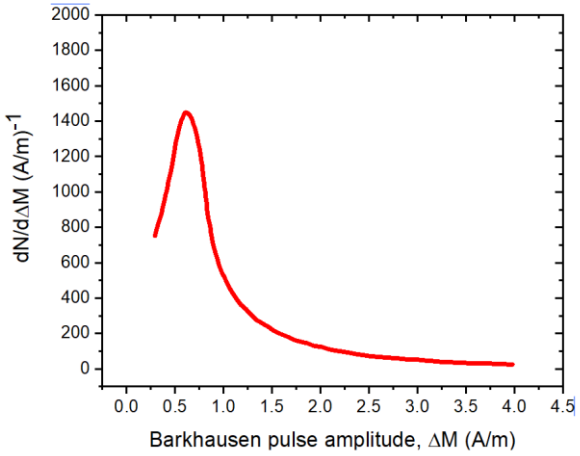

Fig. 9. Magnetic Barkhausen pulse height distribution. This shows on the y-axis the number of Barkhausen events per unit change in magnetization (dN/dM in units of inverse A/m) plotted against on the x-axis the amplitude of the Barkhausen pulses (ΔM (in units of A/m) [23].

The total Barkhausen signal per unit time $\frac{dM_{JS}}{dt}$ can be represented as a product of these terms together with the dimensionless term γ which simply represents the fraction of the irreversible magnetization change which occurs as Barkhausen events,

$$\frac{d\boldsymbol{M}_{JS}}{dt} = \gamma \frac{d\boldsymbol{M}_{irr}}{dH} . \frac{d\boldsymbol{H}}{dt} \tag{40}$$

as described by Mitra and Jiles [24] and Mitra et al. [25]. The term γ can be further subdivided into the number of Barkhausen events N, and the average size of the Barkhausen events $\langle \mathbf{M}_{disc} \rangle$ per unit irreversible change in magnetization, so that

$$\gamma = \frac{d}{d\boldsymbol{M}_{irr}} (N \langle \boldsymbol{M}_{disc} \rangle) \tag{41}$$

This method of analyzing the Barkhausen signals, allows the stochastic model of Bertotti to be used to determine γ with the event size $\langle \mathbf{M}_{disc} \rangle$ and the number of events N which varies in a random manner. This can then be coupled to the differential irreversible susceptibility dM_{irr}/dH obtained from the hysteresis curve, or alternatively from a hysteresis model such as the Preisach model or the model proposed by Jiles and Atherton, to get the rate of change of magnetic field with time.

This article has been accepted for publication in a future issue of this journal, but has not been fully edited. Content may change prior to final publication. Citation information: DOI 10.1109/TMAG.2020.3034208, IEEE Transactions on Magnetics

$$\frac{d\boldsymbol{M}_{JS}}{dt} = \frac{d\boldsymbol{M}_{irr}}{dH} \cdot \frac{d\boldsymbol{H}}{dt} \cdot \frac{d}{d\boldsymbol{M}_{irr}} (N\langle \boldsymbol{M}_{disC} \rangle) \tag{42}$$

The number of Barkhausen events can be obtained from the stochastic Barkhausen model of Bertotti which essentially considers the number of events in each time interval to be a stochastically fluctuating function. The number of events in each time interval obeys a "random walk" which is mathematically equivalent to the description of Brownian motion. From one-time interval to the next, there is a correlation between the number of events. The probability of a Barkhausen event occurring at any given location is low, but there are a very large number of locations. Under these conditions, the behavior follows a Poisson distribution in which the standard deviation of several events N, is simply $\sqrt{N}$. If we suppose that the increment or decrement in the number of events from one period to the next is determined by this standard deviation, then the number of events N_t in the interval t, is related to the number of events N_{t-1} in the previous interval *t*-1 by

$$N_t = N_{t-1} + \delta_{rand}\sqrt{N_{t-1}} \tag{43}$$

where δ_{rand} is a random number lying in the range +/- 1.47[1]. The expression for the Barkhausen activity becomes

$$\frac{d\boldsymbol{M}_{JS}}{dt} = \frac{d\boldsymbol{M}_{irr}}{dH} \cdot \frac{d\boldsymbol{H}}{dt} \cdot \left(N \frac{d\langle \boldsymbol{M}_{disc} \rangle}{d\boldsymbol{M}_{irr}} + \langle \boldsymbol{M}_{disc} \rangle \cdot \frac{dN}{d\boldsymbol{M}_{irr}}\right) \tag{44}$$

Both terms in the parentheses on the right-hand side have a statistical character, however $<M_{disc}>$ the size of the Barkhausen jumps is likely to be only weakly related to the irreversible change in magnetization. On the other hand, for a given distribution of Barkhausen jumps the number of events N is likely to be an approximately linear function of M_{irr}. Therefore, to a good approximation we may expect,

$$\frac{d\boldsymbol{M}_{JS}}{dt} = \frac{d\boldsymbol{M}_{irr}}{dH} \cdot \frac{d\boldsymbol{H}}{dt} \cdot \langle \boldsymbol{M}_{disc} \rangle \cdot \frac{dN}{d\boldsymbol{M}_{irr}} \tag{45}$$

Most Barkhausen activity occurs close to the coercivity $\boldsymbol{H_c}$ where the slope dM/dH of the magnetization curve reaches a maximum. Therefore, for a fixed rate of change of field dH/dt, the rate of change of magnetization with time (dM/dt = (dM/dH)/(dH/dt) reaches a maximum at the coercivity, resulting in more Barkhausen events in a given time interval.

Double peaks in the count rate can occur, particularly if the material is composed of two phases each with a different coercivity as shown by Raghunathan et al. [26]. Also, the location and size of the peaks can shift as a result of changes in the defect distribution, as shown by Theiner et al. in Fig. 10 for two specimens of the same material but with different defect distributions.

This article has been accepted for publication in a future issue of this journal, but has not been fully edited. Content may change prior to final publication. Citation information: DOI 10.1109/TMAG.2020.3034208, IEEE Transactions on Magnetics

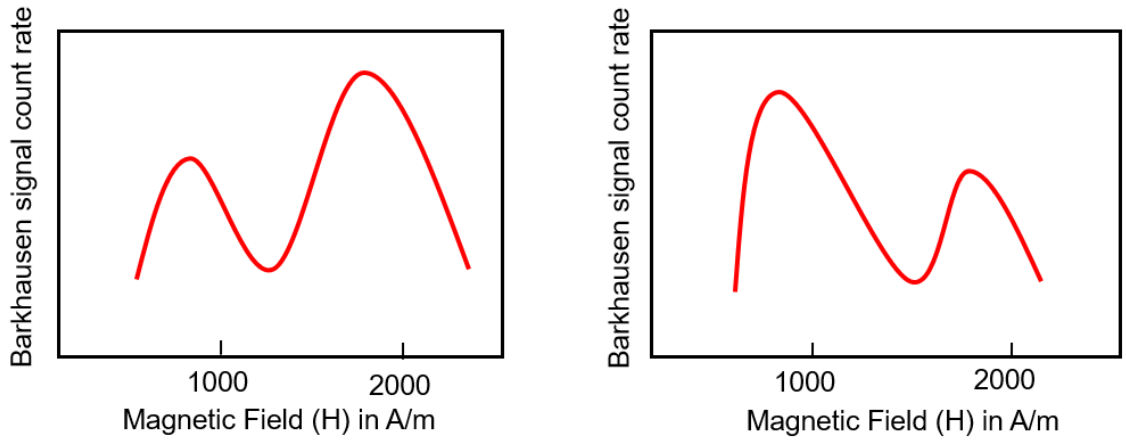

Fig. 10. Barkhausen count rate as a function of magnetic field ***H*** for specimens with two different defect distributions. After Theiner et al. [27, 28].

3.2 APPLICATIONS OF THE BARKHAUSEN EFFECT.

Measured Barkhausen signal amplitude changes with applied and residual stress which make it a useful technique for nondestructive evaluation. As tensile stress increases, the peak Barkhausen amplitude in steel was found to increase as shown in Fig. 11 [29]. However as compressive stress increases it was found that the peak Barkhausen amplitude in steel decreases.These changes can be explained by the extensions to the JA model as described above particularly equations (31) and (42). Investigations by Tiitto [30] reported the effects of elastic and plastic strain on the magnetic Barkhausen emissions (MBE) in silicon-iron and the microstructural dependence of MBE in steels. He was able to show that MBE could be used to determine grain size in steels nondestructively.

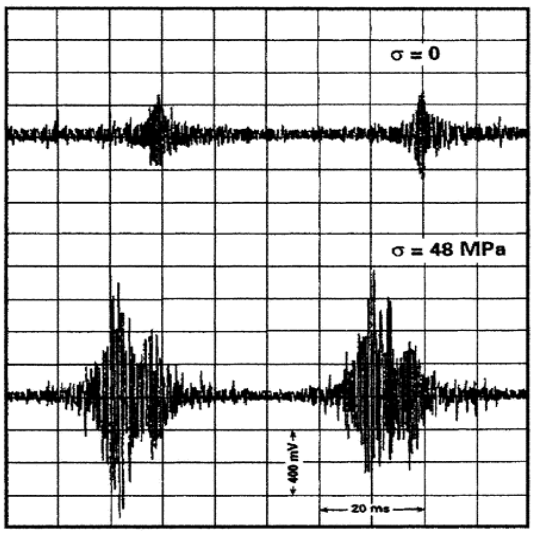

Fig. 11. Measured voltage versus time plots Barkhausen emissions showing changes in Barkhausen emissions with tensile stress in carbon steel, Lo, Kinser and Jiles [29].

The effect of tensile cyclic stress loading on MBE signals during fatiguing of mild steel was the subject of an investigation by Karjalainen et al. [31]. They found that residual strains in unloaded specimens could be identified from the root-mean-square of the MBE signals. But changes occurring under cyclic loading (fatigue cycling) were very complex so that the Barkhausen signals could not simply be related to the applied load. However, Ruuskanen and Kettunen [32] were able to

demonstrate that the median Barkhausen pulse amplitude could be used to assess whether the applied stress amplitude was above or below the fatigue limit.

Lomaev [33] identified five mechanisms by which MBE is caused: (a) discontinuous, irreversible domain-wall motion; (b) discontinuous rotation within a domain; (c) appearance and disappearance of Neel peaks; (d) inversion of magnetization in single-domain particles; and (e) displacement of Bloch or Neel lines in two 180° walls with oppositely directed magnetizations.

The first of these mechanisms has been studied most intensively and is often incorrectly quoted as the sole mechanism for generation of MBE. It is interesting to note that, contrary to this, in the early years of MBE the effect was erroneously attributed largely to the second mechanism, that is irreversible domain rotation.

Barkhausen emissions that are detected on the surface of a test sample originate only from the surface layer. The Barkhausen effect can therefore be used to probe surface plastic deformation of steel components by using measurements at different frequencies that therefore represent properties averaged over different depths. This technique of detecting Barkhausen signals over controlled ranges of frequency can be used for evaluation of different types of surface condition such as case hardening or surface decarburization. A combination of MBE at different frequencies and hysteresis measurements was used by Mayos [34] for the determination of surface decarburization in steels. By this method different depths of the material were inspected to investigate changes in magnetic properties with depth.

Theiner et al. used MBE in conjunction with incremental permeability and ultrasonic measurements for the evaluation of stress. As they noted, ferromagnetic NDE methods are sensitive to both mechanical stress and microstructure of the material. Therefore, in order to determine stress, it is necessary to use two or three independent measurement parameters. They found that Barkhausen effect, incremental permeability, X-ray diffraction and hardness measurements were useful in estimating residual stress. Changes in the density of dislocations affected the detected MBE signals. They also found that MBE could be used to distinguish between different microstructures which cannot be distinguished based on optical microscopy.

Theoretical work by Jiles et al. developed equations for the Barkhausen effect to describe both the stochastic and deterministic component and a model for the stress dependence of the differential susceptibility at different angles to the stress was developed. When combined these resulted in equation (46) in which the reciprocal of the Barkhausen voltage amplitude was linearly proportional to stress [35] according to the following equation

$$\frac{1}{V_{MBE}(\sigma)} = \frac{1}{V_{MBE}(0)} - \frac{3b'\sigma}{\mu_0} \tag{46}$$

where $V_{MBE}(0)$ is the peak Barkhausen voltage under zero stress, $V_{MBE}(\sigma)$ is the peak Barkhausen voltage under stress σ along the applied field direction as shown in Figs. 12 (a) and (b). The coefficient 'b' is an adjustable empirical model parameter that originates from earlier work and links Barkhausen voltage to differential susceptibility, magnetostriction and magnetization, and μ_o is the permeability of free space. This relation has been verified experimentally. Note that equation (46) is analogous to equation (35) which arises due to the close relationship between Barkhausen voltage emissions and differential permeability around the hysteresis loop.

This article has been accepted for publication in a future issue of this journal, but has not been fully edited. Content may change prior to final publication. Citation information: DOI 10.1109/TMAG.2020.3034208, IEEE Transactions on Magnetics

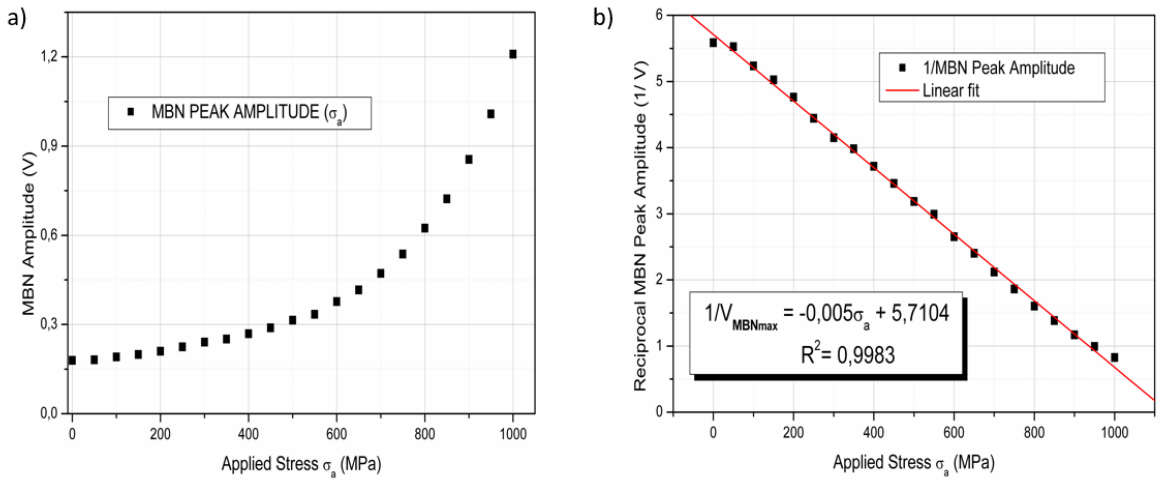

Fig. 12 (a). MBE peak amplitude for carburized SAE 9310 specimen as a function of applied stress and 12 (b). Reciprocal of MBE peak amplitude for carburized SAE 9310 specimen as a function of applied stress. Compare with Figs.4 (a) and (b).

4. CONCLUSION

In this paper, an integrated model has been developed that describes ferromagnetic hysteresis, magneto-mechanical effect and Barkhausen effect properties of magnetic materials. The model is mainly based on the Jiles-Atherton theory and its extensions. It provides a self-consistent set of equations and links model parameters to properties via a conceptual framework that can be used to help determine the model parameters and understand the inter-connections between magnetic properties such as hysteresis, the magnetomechanical effect and the Barkhausen effect. The model can be used to link the model parameters to measured magnetic properties of materials. Understanding the factors which determine the properties and performance of materials is important in design and optimization of devices such as sensors, actuators, electromagnets, electric motors, transformers and generators which utilize ferromagnetic material.

5. REFERENCES

1. Jiles, D.C. and Melikhov, Y., "Modelling of non-linear behavior and hysteresis in magnetic materials" in Handbook of Magnetism and Advanced Magnetic Materials, Volume 2: Micromagnetism, p. 1059-1079, Editors H.Kronmuller and S.S.Parkin, John Wiley & Sons, Scientific Publishers, 2007.
2. Jiles D.C.,"Dynamics of domain magnetization and the Barkhausen effect", Czechoslovak Journal of Physics, 50, 893, 2000.
3. Preisach, F. (1935) Z. *Phys.,* 94, 277.
4. Stoner, E. C. and Wohlfarth, E. P. (1948) *Phil. Trans. Roy. Soc*., A240, 599.
5. Jiles, D. C. and Atherton, D. L. (1986) *J. Mag. Mag. Mater.,* 61, 48.
6. Jiles, D. C. (1994). Frequency dependence of hysteresis curves in conducting magnetic materials. *Journal of Applied Physics*, *76*(10), 5849-5855.
7. Jiles D,C. "Introduction to Magnetism & Magnetic Materials", 3rd edition, p.196, CRC Press, Boc Raton, (2016).
8. Jiles, D. C. and Thoelke, J. B. (1989) Proceedings of the 1989 Intermag Conference, *IEEE Trans. Mag.,* 25, 3928, (1989).
9. Jiles, D. C., Thoelke, J. B. and Devine M.K. (1992) *IEEE Trans. Mag.,* 28, 27.
10. Jiles, D. C. (1988) *J. Phys. D.* (*Appl. Phys.*), 21, 1196.
11. Sablik, M. J., Kwun, H., Burkhardt, G. L. and Jiles, D. C. (1988) *J. Appl. Phys.,* 63, 3930.

12. Garikepati, P., Chang, T.T. and Jiles D.C, "Theory of Ferromagnetic Hysteresis : Evaluation of Stress from Hysteresis Curves", IEEE Trans. Magn., 24, 2922, 1988
13. Kaminski, D. A., Jiles, D. C. and Sablik, M. J. (1992) *JMMM,* 104, 382.
14. Jiles, D.C., "Theory of the magnetomechanical effect", Journal of Physics D (Applied Physics), 28, 1537, 1995.
15. Shah, M. B. and Bose, M. S. C. (1984) *Phys. Stat. Solidi.,* 86, 275.
16. Barkhausen, H. (1919) *Phys. Z.,* 29, 401.
17. Prabhu Gaunkar, N. "Magnetic hysteresis and Barkhausen noise emission analysis of magnetic materials and composites". MS, Iowa State University, 2014.
18. Schroeder, K. and McClure, J. C. (1976) The Barkhausen effect, *CRC Critical Reviews of Solid State Science*, 6, 45.
19. Alessandro, B., Beatrice, C., Bertotti, G. and Montorsi, A. (1990) *J. Appl. Phys.,* 68, 2901.
20. Jiles, D. C., Sipahi, L. B., & Williams, G. (1993). Modeling of micromagnetic Barkhausen activity using a stochastic process extension to the theory of hysteresis. *Journal of applied physics*, *73*(10), 5830-5832.
21. Matzkanin, G. A., Beissner, R. E. and Teller, C. M. (1979) *SWRI Report No. NTIAC-79-2*
22. Jiles, D. C., and Suominen, L. (1994). "Effects of surface stress on barkhausen effect emissions: Model predictions and comparison with x-ray diffraction studies". *IEEE transactions on magnetics*, *30*(6), 4924-4926.
23. Jiles, D.C., "Review of magnetic methods for nondestructive evaluation", Nondestructive Testing International, 21, 311, 1988, after Tebble R.S., Skidmore and Corner W.D., Proc. Phys. Soc. A63, p.739, (1950)
24. Mitra, A., & Jiles, D. C. (1997). Magnetic Barkhausen emissions in as-quenched FeSiB amorphous alloy. *Journal of magnetism and magnetic materials*, *168*(1-2), 169-176.
25. A. Mitra, Z. J. Chen, F. Laabs & D. C. Jiles (1997) Micromagnetic Barkhausen emissions in 2·25 wt% Cr–1 wt% Mo steel subjected to creep, Philosophical Magazine A, 75:3, 847-859
26. Raghunathan, A., Melikhov, Y., Snyder, J.E. and Jiles, D.C, J. Mag. Mag. Mater., 324, 20, 2012.
27. Theiner, W. A. and Altpeter, I. (1983) in *New Procedures in NDT* (ed. P. Holler), Springer-Verlag, Berlin.
28. Schneider, E., Theiner, W. A. and Altpeter, I. (1984) in *Nondestructive Methods for Materials Property Determination* (eds C.O. Ruud & R.E. Green), Plenum Press, New York
29. Lo C.C.H., Kinser E.R. and Jiles, D.C., "Analysis of Barkhausen effect signals in surface-modified magnetic materials using a hysteretic-stochastic model", J. Appl. Phys., 99, 08B705, 2006.
30. Tiitto, S. (1977) *Acta Polytechnica Scand.,* 119, 1, 1977
31. Karjalainen, L. P., Moilanen, M. and Rautioaho, R. (1979) *Mater. Eval.,* 37, 45.
32. Ruuskanen P, and Kettunen P.O. NDT International, 13, 105, 1980.
33. Lomaev, G. V., Malyshev, V. S. and Degterev, A. P. (1984) Sov. *J. NDT,* 20, 189.
34. Mayos, M., Segalini, S. and Putignani, M. (1987) in *Review of Progress in Quantitative NDE* (eds D. O. Thompson and D. E. Chimenti), Plenum Press, New York.
35. Mierczak L., Jiles, D.C., and Fantoni G., "A New Method for Evaluation of Mechanical Stress Using the Reciprocal Amplitude of Magnetic Barkhausen Noise", IEEE Transactions on Magnetics, 47, 459, 2011.